European Journal of Neuroscience, pp. 1–9, 2007 doi:10.1111/j.1460-9568.2007.05549.x

Similar GABAergic inputs in dentate granule cells born during embryonic and adult neurogenesis

Diego A. Laplagne,[1,*] Juan E. Kamienkowski,[1,*] M. Soledad Espósito,[1] Verónica C. Piatti,[1] Chunmei Zhao,[2] Fred H. Gage[2] and Alejandro F. Schinder[1]
[1]Laboratorio de Plasticidad Neuronal, Fundación Instituto Leloir (1405) Buenos Aires, Argentina
[2]Laboratory of Genetics, The Salk Institute for Biological Studies, La Jolla, CA 92037, USA

Keywords: development, hippocampal slices, inhibition, mouse, whole-cell recordings

Abstract

Neurogenesis in the dentate gyrus of the hippocampus follows a unique temporal pattern that begins during embryonic development, peaks during the early postnatal stages and persists through adult life. We have recently shown that dentate granule cells born in early postnatal and adult mice acquire a remarkably similar afferent connectivity and firing behavior, suggesting that they constitute a homogeneous functional population [Laplagne *et al.* (2006) *PLoS Biol.*, 4, e409]. Here we extend our previous study by comparing mature neurons born in the embryonic and adult hippocampus, with a focus on intrinsic membrane properties and γ-aminobutyric acid (GABA)ergic synaptic inputs. For this purpose, dividing neuroblasts of the ventricular wall were retrovirally labeled with green fluorescent protein at embryonic day 15 (E15), and progenitor cells of the subgranular zone were labeled with red fluorescent protein in the same mice at postnatal day 42 (P42, adulthood). Electrophysiological properties of mature neurons born at either stage were then compared in the same brain slices. Evoked and spontaneous GABAergic postsynaptic responses of perisomatic and dendritic origin displayed similar characteristics in both neuronal populations. Miniature GABAergic inputs also showed similar functional properties and pharmacological profile. A comparative analysis of the present data with our previous observations rendered no significant differences among GABAergic inputs recorded from neurons born in the embryonic, early postnatal and adult mice. Yet, embryo-born neurons showed a reduced membrane excitability, suggesting a lower engagement in network activity. Our results demonstrate that granule cells of different age, location and degree of excitability receive GABAergic inputs of equivalent functional characteristics.

Introduction

The dentate gyrus constitutes the main gateway to the mammalian hippocampus (Johnston & Amaral, 1998). Its principal neurons, the dentate granule cells (DGCs), receive their main inputs from the entorhinal cortex and project onto CA3 pyramidal cells and a variety of local interneurons. The development of the mouse and rat dentate gyrus has been described in depth (Angevine, 1965; Schlessinger *et al*., 1975, 1978; Bayer, 1980; Altman & Bayer, 1990a,b). While input and output neurons that connect to DGCs are largely generated before birth, the generation of DGCs follows a unique temporal pattern that begins at about embryonic day 14 (E14) and persists throughout life (Schlessinger *et al*., 1978). All DGCs ultimately derive from precursors generated in the primary dentate neuroepithelium, located on the medial wall of the lateral ventricle (Altman & Bayer, 1990b).

A proportion of these precursors become postmitotic as early as E14, and their progeny migrate toward the external shell of the outer blade (Schlessinger *et al*., 1975). An adjacent secondary dentate matrix forms by E18 from which proliferating neuroblasts migrate to complete the outer shell of the granule cell layer (GCL). A tertiary dentate matrix is formed in the hilar region at around birth, from which a large number of DGCs (about 80%) are postnatally generated (Schlessinger *et al*., 1975; Bayer, 1980; Altman & Bayer, 1990a). After the first 2 weeks of life, proliferation is largely restricted to the subgranular zone, the neurogenic niche that will continuously generate DGCs throughout life.

This unique spatiotemporal pattern of neurogenesis opens the question of whether DGCs generated at those different developmental stages will share a similar functionality in the adult brain. Early observations addressing this issue came from Wojtowicz and colleagues, who found that glutamatergic synapses onto neurons from the inner GCL are more likely to undergo long-term potentiation (Wang *et al*., 2000; Snyder *et al*., 2001). Indeed, entorhinal afferents impinging onto immature neurons of the adult dentate gyrus were later shown to have a lower threshold for the induction of long-term potentiation when compared with mature DGCs (Schmidt-Hieber *et al*., 2004). More recently we and others have shown that, while developing, adult-born DGCs display a radically different morphology, membrane properties and input connectivity compared with mature granule neurons (Espósito *et al*., 2005; Ge *et al*., 2006; Overstreet-Wadiche *et al*., 2006; Piatti *et al*., 2006; Zhao *et al*., 2006). It has remained elusive whether mature neurons born in the adult brain are functionally different from neighboring cells generated during perinatal development. This question represents a technical challenge: while the inside-out addition of DGCs results in an apparent

Correspondence: Dr A.F. Schinder, as above.
E-mail: aschinder@leloir.org.ar
*D.A.L. and J.E.K. contributed equally to this work.

Received 22 November 2006, revised 8 March 2007, accepted 20 March 2007

correlation of cell birth date and localization in the GCL, the high amount of spatial overlapping makes unambiguous birth dating difficult (Angevine, 1965; Schlessinger *et al.*, 1975). This problem can be overcome by specifically labeling cells born at different ages.

In a recent work, we labeled dividing progenitor cells in the early postnatal (P7) and adult (P42) dentate gyrus in the same mice, using two retroviruses expressing different fluorescent proteins (Laplagne *et al.*, 2006). We performed electrophysiological recordings from both neuronal populations in the same slices, and compared their afferent connectivity and membrane properties. We found a remarkable similarity in the excitatory and inhibitory inputs onto these cells, and concluded that all DGCs generated in the postnatal brain are part of a common functional population. As stated above, however, about 20% of DGCs are born before birth and originate from the primary and secondary dentate matrices, while postnatal cells would arise mostly from the tertiary dentate matrix in the hilus and from neuroblasts in the subgranular zone. The possibility still remains that neurons generated pre- and postnatally contribute to different functional populations. In this work, dividing neuroblasts were labeled in murine embryos at E15 by ventricular injection of a retrovirus expressing green fluorescent protein (GFP). A red fluorescent protein (RFP)-expressing retrovirus was injected in the same mice at P42 to label adult-generated neurons. We carried out an extensive comparison of γ-aminobutyric acid (GABA)ergic inhibitory postsynaptic currents (IPSCs) and intrinsic membrane properties. Our results show that all DGCs converge to a remarkably similar pattern of afferent connectivity.

Materials and methods

Viral vectors

A replication-deficient retroviral vector based on the Moloney murine leukemia virus was used to express enhanced GFP or mRFP1 (RFP; Campbell *et al.*, 2002) driven by a CAG promoter (Laplagne *et al.*, 2006; Zhao *et al.*, 2006). Retroviral particles were assembled using three separate plasmids containing the capside (CMV-vsvg), viral proteins (CMV-gag/pol) and transgene (CAG-GFP or CAG-RFP). Plasmids were transfected onto 293T cells using Lipofectamine 2000 (Invitrogen, Carlsbad, CA, USA). Virus-containing supernatant was harvested 48 h after transfection and concentrated by two rounds of ultracentrifugation.

Subjects and stereotaxic surgery

For injection of E15 embryos, timed pregnant C57Bl/6J mice were anesthetized (80 μg ketamine/8 μg xylazine in 8 μL saline/g) and the uterus was exposed through a ventral laparotomy. A sharp glass micropipette was guided by hand into the left or right ventricle of the embryos through the uterine wall, and 1 μL of CAG-GFP retroviral suspension was pressure injected. Fast green (Sigma, St. Louis, Missouri, USA) was co-injected to assess proper localization of the inoculum. All embryos in the uterus were usually injected. The peritoneal cavity was irrigated with warm sterile NaCl 0.9% throughout the procedure. The peritoneum and skin incisions were subsequently sutured. Surviving mice were anesthetized at P42–49 (100 μg ketamine/10 μg xylazine in 10 μL saline/g), and a second surgery was carried out to infuse the CAG-RFP retrovirus (0.7 μL in 5 min) into the dorsal aspect of the right dentate gyrus (coordinates: anteroposterior: −2 mm from bregma; lateral: 1.5 mm; ventral: 1.9 mm). Three days before the second surgery and thereafter mice were housed with a running wheel to increase the efficiency of viral transduction (van Praag *et al.*, 2002; Espósito *et al.*, 2005; Laplagne *et al.*, 2006). For measurement of miniature IPSCs (mIPSCs), a single injection with the CAG-GFP retrovirus was performed at P42–49 to label adult-born neurons, as described for the second surgery. Housing and procedures were carried out according to NIH guidelines and approved by the Ethics and Biosafety Committee of the Leloir Institute.

Immunofluorescence and confocal microscopy

Double-labeling of GFP and RFP was analysed in 400-μm horizontal sections cut with a vibratome and fixed with 4% paraformaldehyde. Antibodies were applied in Tris-buffered saline with 3% donkey serum and 0.25% Triton X-100. Primary antibody: NeuN (mouse monoclonal; 1 : 50). Secondary antibody: donkey anti-mouse Cy5 (1 : 250, Jackson ImmunoResearch, West Grove, PA, USA). Images were taken using a Zeiss Pascal confocal microscope.

Electrophysiology

Experiments on evoked IPSCs (eIPSCs) and spontaneous IPSCs (sIPSCs) were carried out in 29 slices from 14 mice injected at E15 and P42 (eight male, six female), 6.7 ± 0.4 weeks (range: 6.0–7.6) after the second (P42) surgery. Experiments on mIPSCs were carried out in 50 slices from 27 female mice, 7.0 ± 0.7 weeks (range: 5.7–8.1) after the retroviral injection. Mice were anesthetized and decapitated. Brains were removed into a chilled solution containing (in mM): choline-Cl^-, 110; KCl, 2.5; NaH_2PO_4, 2; $NaHCO_3$, 25; $CaCl_2$, 0.5; $MgCl_2$, 7; dextrose, 20; Na^+-ascorbate, 1.3; Na^+-pyruvate, 0.6; kynurenic acid (kyn), 4. Right hemisphere horizontal slices (400 μm thick) were cut in a vibratome and transferred to a chamber containing artificial cerebrospinal fluid (ACSF; in mM): NaCl, 125; KCl, 2.5; NaH_2PO_4, 2; $NaHCO_3$, 25; $CaCl_2$, 2; $MgCl_2$, 1.3; Na^+-ascorbate, 1.3; Na^+-pyruvate, 3.1; dextrose, 10. Stereotaxic injections mostly labeled dorsal DGCs. Slices were bubbled with 95% O_2/5% CO_2 (315 mOsm) and maintained at 30 °C. Recordings were carried out in ACSF containing 4 mM kyn at 24 ± 1 °C using microelectrodes (3–5 MΩ) pulled from borosilicate glass (KG-33, Garner Glass, Claremont, CA, USA). Three internal solutions were used, all of them included (in mM): Hepes, 10; Tris-ATP, 4; Tris-GTP, 0.3; phosphocreatine, 10; and Alexa Fluor 488 or 594 (10 μg/mL; Invitrogen), pH 7.3 and 290 mOsm. Internal solutions used for recordings of eIPSCs and intrinsic membrane properties also included (in mM): Kgluconate, 120; KCl, 20; NaCl, 5; $MgCl_2$, 4; EGTA, 0.1. For sIPSCs recorded at a holding potential (V_{Hold}) of −80 mV and mIPSCs we included (in mM): Kgluconate, 19; KCl, 121; NaCl, 5; $MgCl_2$, 4; EGTA, 0.1. For sIPSCs at $V_{Hold} = 0$ mV we included (in mM): CsCl, 140; NaCl, 5; $MgCl_2$, 2; EGTA, 0.1. Tetrodotoxin (TTX) was from Alomone Laboratories (Jerusalem, Israel). Zolpidem hemitartrate was a generous gift from Dr D. Calvo. Unless otherwise noted, all other chemicals were from Sigma.

Whole-cell recordings (Axopatch 200B, Molecular Devices, Sunnyvale, CA, USA) were filtered, digitized and acquired onto a PC using jClamp (SciSoft [http://www.scisoftco.com/jclamp.html]). Passive properties were analog filtered at 10 kHz and digitized at 50 kHz, for eIPSCs we used 2 kHz/20 kHz, and for sIPSCs and mIPSCs we used 2 kHz/10 kHz. Series resistance was typically 15–25 MΩ. Criteria to include cells in the analysis were: (1) co-labeling with Alexa Fluor 594 (for GFP^+ cells) or 488 (for RFP^+ cells), or visual confirmation of GFP or RFP fluorescence in the pipette tip; and (2) absolute leak current < 150 pA. Extracellular stimulation (50 μs, 0.1 Hz) was done using concentric bipolar electrodes (50 μm diameter; FHC, Bowdoinham, Maine, USA). In paired experiments,

a development-born DGC (GFP^+) and one neighboring adult-born DGC (RFP^+) were sequentially recorded while maintaining electrode position, stimulation protocols and stimulus strength (mostly 10 V, 50 μs) invariable. The order in which GFP^+ and RFP^+ cells were recorded was alternated across experiments. The stimulation electrode was positioned on the GCL or outer third of the molecular layer (ML), as stated in the text, and ~250 μm away from the recorded cell. When more than one DGC of the same group was recorded for the same paired experiment, average values were used for comparisons. E15-born DGCs of the outer half of the GCL were selected for electrophysiological recordings (Angevine. 1965; Schlessinger *et al*., 1975). The threshold current for action potentials was measured as the minimal step required to observe a spike in current-clamp. The baseline membrane potential was maintained at −80 mV by injecting a constant current. Action potential threshold was measured as the membrane voltage at the onset of the spike.

mIPSCs were measured at $V_{Hold} = -60$ mV in the presence of 0.5 μM TTX (Hollrigel & Soltesz, 1997; Stell & Mody, 2002). Complete blockade of action potentials was confirmed in each experiment. For these experiments, unlabeled (GFP^-) DGCs of the outer third of the GCL were taken as development-born (Mathews *et al*., 2006). In additional support of this criterion, it has been shown that adult-born neurons largely remain within the inner third of the GCL (Kempermann *et al*., 2003; Espósito *et al*., 2005).

Analysis of electrophysiological data

Passive properties were calculated from the current response to a 10-mV hyperpolarizing step; series and input resistances were measured from the peak and steady-state values of the negative deflection. Membrane capacitance was obtained from the area under the capacitive current. Evoked postsynaptic currents were analysed from average traces using ad-hoc MATLAB routines (The Mathworks [http://www.mathworks.com/products/matlab]). For ML-evoked currents, the GABA reversal potential E_{GABA} and the slope conductance G_{GABA} were calculated from *I–V* curves constructed at the time of the outward IPSC peak (Fig. 2C). For GCL-evoked currents, E_{GABA} and G_{GABA} were calculated from *I–V* curves constructed at two time points: (1) the peak of the IPSC at $V_{Hold} = -80$ mV ('early'); and (2) 145 ms after the stimulation artifact ('late'; Fig. 2D). In some experiments, the current amplitude at $V_{Hold} = -80$ mV deviated from linearity and was not considered for the *I–V* fitting. Rise and decay times were calculated from 20–80% and 100–40% of the peak amplitude, respectively. For individual sIPSCs recorded at 0 mV (Fig. 3F) decay time represents the time constant from single-exponential fits of the decay phase. All example traces of evoked responses are averages of > 10 sweeps.

sIPSCs and mIPSCs were sampled with Axoscope 9 (Molecular Devices), digitally filtered at 1 kHz, and detected offline with Mini Analysis software (Synaptosoft, [http://www.synaptosoft.com/MiniAnalysis]). Amplitude and area thresholds for detection were 10 pA and 50 pA/ms (sIPSCs) or 20 pA/ms (mIPSCs), and the average standard deviation of baseline noise was 2 pA. All events were individually validated, and artifacts were discarded by visual inspection. For analysis of sIPSC and mIPSC peak amplitude, a mean value was obtained for each DGC. Individual sIPSCs were then exported to MATLAB where kinetics were analysed and two-dimensional histograms were obtained using routines developed in our laboratory. Kinetics were analysed from the scaled average event from each cell. mIPSCs with slow decay (> 40 ms, less than 1% of all events) or small amplitude (< 20 pA) were not included in the kinetic analysis. For the construction of scaled averages, traces were aligned at 10% of the rising phase and events with multiple peaks were discarded. In the pharmacological experiments shown in Fig. 3C and D, no spontaneous events were detected in recordings lasting about 3 min for each cell in the presence of bicuculline (BMI). All statistical tests used two-tailed analysis.

Results

Retroviral labeling of DGCs

We have recently shown that double retroviral injections can be successfully used to express different fluorescent proteins for unambiguous labeling of neurons born in the early postnatal and adult hippocampus (Laplagne *et al*., 2006). In the present work we have adapted the technique to label DGCs generated in the embryonic and adult hippocampus. To identify DGCs born during embryonic development, a retrovirus encoding GFP was delivered to the ventricle of E15 murine embryos through intrauterine injections. Seven weeks after birth, the same mice received a stereotaxic injection of a retrovirus encoding RFP to label adult-born neurons. Hippocampal slices obtained from these mice contained both GFP^+ and RFP^+ neurons, with adult-born cells positioned deeper in the GCL (Fig. 1), consistent with the known spatiotemporal pattern of neurogenesis in the dentate gyrus (Angevine, 1965; Kempermann *et al*., 2003; Espósito *et al*., 2005). Acute hippocampal slices were used for the electrophysiological studies described below.

Evoked GABAergic inputs

Intracellular recordings from principal neurons allow for the distinction of the two main classes of GABAergic inputs: somatic and dendritic (Pearce, 1993; Soltesz *et al*., 1995). Perisomatic GABAergic responses are preferentially evoked by stimulation of interneurons in the GCL and display fast kinetics. Dendritic responses are best evoked by stimulation of the ML and are much slower, possibly owing to electrotonic filtering and differences in $GABA_A$ receptor composition (Pearce, 1993; Soltesz *et al*., 1995; Espósito *et al*., 2005; Laplagne *et al*., 2006). Furthermore, the Cl^- concentration at or near the soma is imposed by the patch pipette, while incomplete diffusion and active local transport result in a concentration gradient towards the dendrites (Jarolimek *et al*., 1999). As the reversal potential of IPSCs (E_{GABA}) is largely determined by the Nernst equilibrium potential of Cl^- at the postsynaptic site (Kaila, 1994), E_{GABA} can be used to determine the subcellular origin of GABAergic inputs (Pearce, 1993; Espósito *et al*., 2005; Laplagne *et al*., 2006).

Synaptic inputs from inhibitory interneurons onto embryo-born DGCs were studied in hippocampal slices obtained from 13-week-old mice by extracellular stimulation of the outer ML and the GCL in the presence of the ionotropic glutamate receptor antagonist kyn (4 mM; Fig. 2A). Synaptic currents evoked by these protocols were mediated by $GABA_A$ receptors as they were completely and reversibly blocked by 20 μM BMI (Fig. 2B). Stimuli delivered to the ML evoked slow responses with a hyperpolarized E_{GABA}, underlining their dendritic nature (Fig. 2C). In contrast, stimulation of the GCL elicited complex postsynaptic currents dominated by a fast component ('early') bearing a depolarized E_{GABA} that is close to the predicted equilibrium potential for Cl^- in our recoding condition (about −35 mV). This fast current was followed by a slower component ('late') with a more negative reversal potential (Fig. 2D). The statistical significance observed for the values obtained for E_{GABA} evidences different somatodendritic localizations of eIPSCs: perisomatic (early GCL),

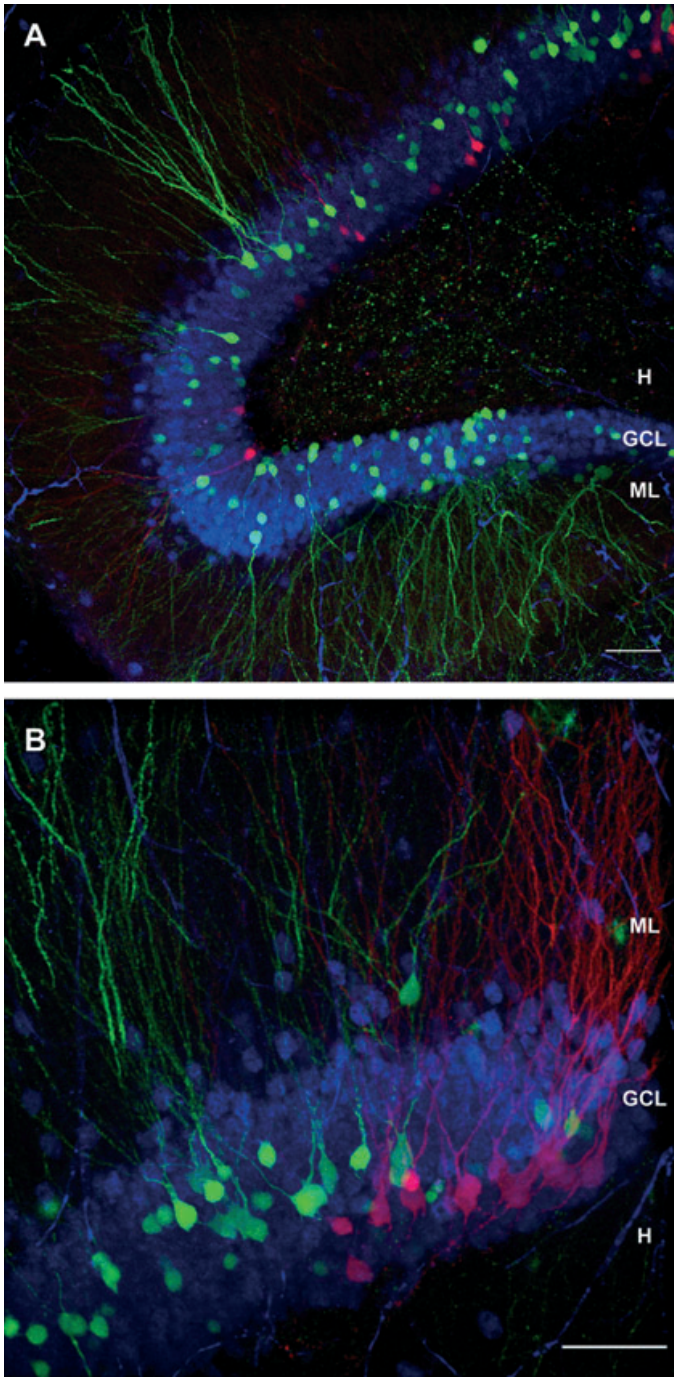

FIG. 1. Fluorescent labeling of DGCs born during embryonic and adult neurogenesis. Double retroviral labeling of DGCs generated at E15 (GFP^+, green) and P42 (RFP^+, red). Images are merges of (A) 16 and (B) 30 confocal planes taken from fixed transverse sections of the dentate gyrus (400 μm thick) from 13-week-old mice. The granule cell layer (GCL) was labeled by immunohistochemistry for the neuronal marker NeuN (blue). H, hilus; ML, molecular layer. Scale bars: 50 μm.

proximal dendritic (late GCL) and distal dendritic (ML; Fig. 2E). Kinetics of postsynaptic currents recorded in response to stimulation of the GCL and ML varied accordingly (Fig. 2F).

To compare proximal GABAergic inputs we carried out paired experiments in which a neuron born in the embryo (GFP^+) and adult hippocampus (RFP^+) were recorded successively, while maintaining the position and strength of the extracellular stimulus. No significant differences were found in the peak amplitude of IPSCs recorded at −80 mV (Fig. 2G). When comparing results on perisomatic and dendritic IPSCs evoked on embryo-born DGCs with data from pup- and adult-born cells no significant differences were found in peak amplitude, kinetics, whole-cell reversal potential and conductance, strongly suggesting that neurons born at all ages share a common afferent connectivity from GABAergic interneurons (Table 1).

Spontaneous GABAergic currents

Inhibitory afferents from embryo-born neurons (GFP^+) were further characterized by studying spontaneous synaptic activity in the presence of kyn. To separately study sIPSCs arising at the dendritic and perisomatic domains we took advantage of the Cl^- gradient imposed by the patch pipette. Under conditions of symmetrical Cl^-, the predicted reversal potential for perisomatic sIPSCs is 0 mV while that of dendritic events would be shifted to more hyperpolarized values (Laplagne *et al.*, 2006). As expected, while recordings at $V_{Hold} = -80$ mV were dominated by fast perisomatic events (Fig. 3A, E, G and I), recordings at $V_{Hold} = 0$ mV rendered only slow outward sIPSCs (Fig. 3B, F, H and I). All postsynaptic events were completely blocked by BMI, confirming that they are mediated by $GABA_A$ receptors (Fig. 3C and D). Events recorded at each condition also differed significantly in their frequency and kinetics (Fig. 3I). To put these results in the context of our previous observations, we compared the parameters reported here with those measured from DGCs born in the postnatal and adult brain (Laplagne *et al.*, 2006). No significant differences were found in the frequency, peak amplitude and kinetics of both perisomatic and dendritic sIPSCs, further confirming the remarkable similarity of inhibitory afferent connectivity in neurons born in the embryonic, early postnatal and adult hippocampus (Table 1).

Miniature GABAergic currents

To refine the comparison of GABAergic inputs we recorded mIPSCs in the presence of kyn (4 mM) and TTX (0.5 μM) (Fig. 4A). For these experiments, unlabeled cells of the outer third of the GCL were selected as DGCs born during development (see Materials and methods). mIPSCs recorded from neurons born in the developing and adult hippocampus were virtually indistinguishable, as they displayed similar kinetics, amplitude and frequency (Fig. 4B–F). We next examined the effect of the benzodiazepine agonist zolpidem, which is known to prolong the decay phase of GABAergic postsynaptic currents depending on the $GABA_A$ receptor subunit composition (De Koninck & Mody, 1994). The effect of zolpidem has been shown to be more potent in DGCs from the adult than in those from the early postnatal hippocampus (Hollrigel & Soltesz, 1997). Interestingly, $GABA_A$ receptors on immature DGCs of the adult hippocampus lack the α_1 subunit and are insensitive to zolpidem (Overstreet Wadiche *et al.*, 2005). We thus investigated whether this feature is maintained in adult-born neurons after reaching maturity. We observed a similar dose-dependent increase in the decay time of mIPSCs in mature neurons generated both in the developing and adult dentate gyrus, with a slightly larger effect in adult-born neurons (Fig. 4G). Altogether, these observations strengthen the notion that GABAergic transmission onto neurons born during development and adulthood has similar functional properties.

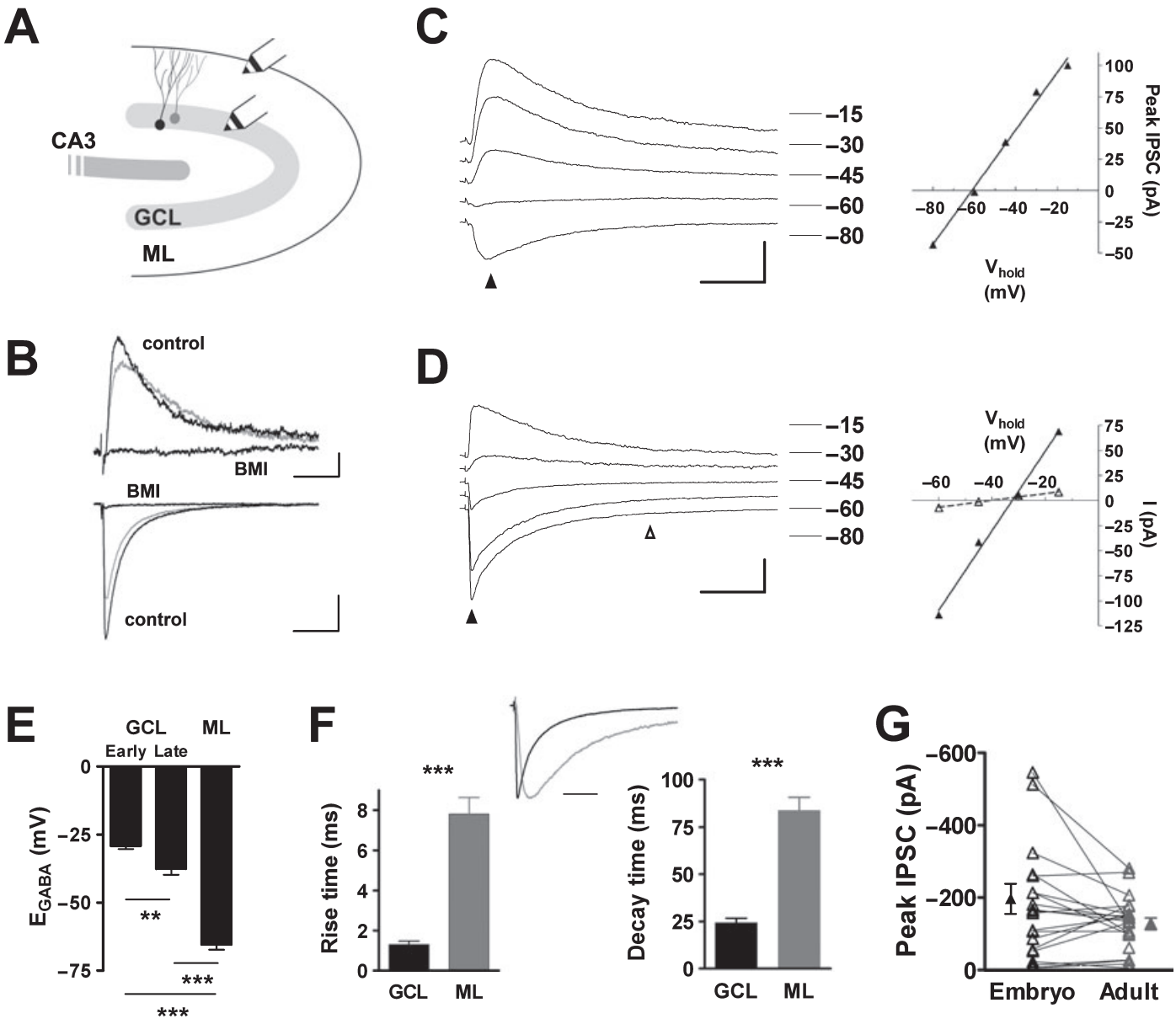

FIG. 2. Evoked GABAergic inputs. (A) Diagram of the dentate gyrus showing typical positions of extracellular stimulation electrodes on the granule cell layer (GCL) and molecular layer (ML). (B) Example recordings of inhibitory postsynaptic currents (IPSCs) evoked by stimulation of the ML (top traces, embryo-born DGC, $V_{Hold} = -30$ mV) and GCL (bottom traces, embryo-born DGC, $V_{Hold} = -80$ mV) displaying reversible blockade by 20 μM bicuculline (BMI); gray traces depict drug washout. GCL-evoked IPSCs were blocked by 97.1 ± 0.4% ($n = 3$), and ML-evoked IPSCs were blocked by 98.5 ± 1.5% ($n = 3$). Scale bars: 50 ms, 5 pA (top) and 25 pA (bottom). (C) Left: average IPSCs in response to ML stimulation on an embryo-born neuron recorded at different holding potentials, as indicated on the right. Right: *I–V* curve measured for the same experiment at the time indicated by the arrowhead. Scale bars: 50 ms, 50 pA. (D) Left: IPSCs in response to GCL stimulation on an embryo-born neuron. Right: *I–V* curves measured for the same experiment at an early time (filled arrowhead) and a late time (open arrowhead). Scale bars: 50 ms, 50 pA. (E) Mean reversal potential of IPSCs evoked by GCL stimulation (measured at early and late times), and ML stimulation on embryo-born neurons (ANOVA: $P < 0.0001$; $n = 11$ GCL, $n = 10$ ML; Bonferroni *post hoc* tests, $^{**}P < 0.01$; $^{***}P < 0.001$). (F) Kinetics of IPSCs evoked by GCL ($V_{Hold} = -80$ mV) and ML ($V_{Hold} \sim -40$ mV) stimulation on embryo-born DGCs (rise time: $P < 0.0001$; decay time: $P < 0.0001$). Inset: normalized average traces of all IPSCs evoked by GCL (black trace) and ML stimulation (gray trace) on embryo-born cells. Scale bar: 50 ms. (G) Peak amplitude of IPSCs evoked by GCL stimulation at $V_{Hold} = -80$ mV on embryo- vs adult-born neurons. Each line connects pairs of values collected in the same experiment. Paired *t*-test rendered no significant differences ($P = 0.09$). Mean ± SEM values are shown on the sides. All experiments were carried out in the presence of 4 mM kyn.

Reduced excitability of DGCs born in the embryonic hippocampus

Intrinsic membrane properties of neurons influence the integration of their synaptic inputs which, in turn, determines their output to the network. We have studied passive and active properties of DGCs born in the embryonic brain. Capacitance and input resistance were measured from the current response to a hyperpolarizing voltage step of 10 mV. Current and voltage threshold for action potentials were measured in response to increasing depolarizing current steps. Interestingly, three-way comparisons between cells born at different stages revealed significant differences in capacitance, input resistance

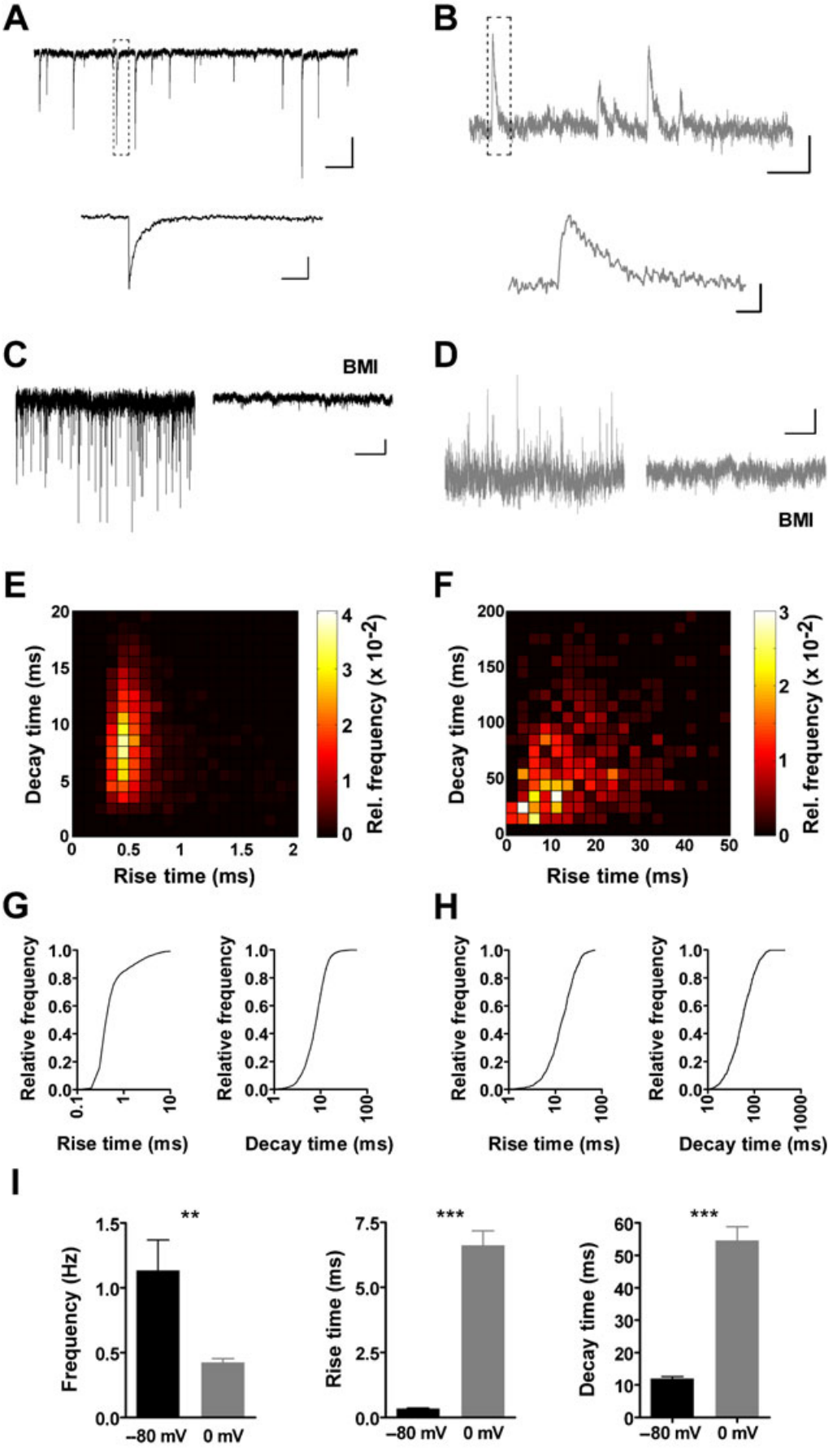

TABLE 1. Statistical analysis of properties measured for embryo-, pup- and adult-born DGCs

	Embryo	Pup*	Adult*	*P*-value[a]
GCL-IPSCs				
Peak amplitude (pA)	−199 ± 42 (21)	−138 ± 30 (19)	−133 ± 17 (40)	0.20
Rise time (ms)	1.32 ± 0.15 (19)	1.46 ± 0.18 (22)	1.80 ± 0.22 (39)	0.26
Decay time (ms)	26.8 ± 2.8 (21)	39.9 ± 4.4 (22)	32.8 ± 3.2 (40)	0.07
E_{GABA} early (mV)	−32.2 ± 3.2 (12)	−29.8 ± 1.4 (11)	−29.2 ± 1.2 (16)	0.55[b]
E_{GABA} late (mV)	−40.3 ± 3.5 (12)	−41.8 ± 3.0 (11)	−41.6 ± 1.9 (16)	0.92
G_{GABA} early (nS)	5.26 ± 0.99 (12)	4.08 ± 0.84 (11)	4.25 ± 0.63 (16)	0.56[c]
G_{GABA} late (nS)	0.45 ± 0.10 (12)	0.53 ± 0.09 (11)	0.44 ± 0.08 (16)	0.72
ML-IPSCs				
E_{GABA} (mV)	−65.4 ± 1.9 (10)	−67.5 ± 1.8 (7)	−66.4 ± 1.7 (11)	0.75
G_{GABA} (nS)	1.35 ± 0.26 (11)	1.48 ± 0.54 (7)	0.94 ± 0.17 (15)	0.36
Rise time (ms)	7.8 ± 0.8 (12)	8.7 ± 1.2 (6)	9.0 ± 1.0 (14)	0.64
Decay time (ms)	83.7 ± 7.0 (12)	77.8 ± 19.5 (6)	80.0 ± 7.7 (14)	0.92
sIPSC −80 mV				
Frequency (Hz)	1.13 ± 0.23 (10)	1.40 ± 0.25 (12)	1.40 ± 0.14 (15)	0.60
Amplitude (pA)	−50.4 ± 3.9 (10)	−43.5 ± 3.9 (12)	−40.0 ± 2.5 (15)	0.11
Rise time (ms)	0.34 ± 0.03 (10)	0.39 ± 0.03 (12)	0.39 ± 0.02 (15)	0.28
Decay time (ms)	12.0 ± 0.6 (10)	13.4 ± 1.2 (12)	13.8 ± 0.6 (15)	0.27
sIPSC 0 mV				
Frequency (Hz)	0.42 ± 0.03 (11)	0.32 ± 0.05 (10)	0.33 ± 0.05 (16)	0.30
Amplitude (pA)	17.8 ± 1.0 (11)	18.4 ± 1.4 (10)	16.8 ± 0.6 (14)	0.47
Rise time (ms)	6.6 ± 0.6 (11)	6.3 ± 0.2 (10)	7.2 ± 0.8 (14)	0.61
Decay time (ms)	54.6 ± 4.2 (11)	48.1 ± 2.7 (10)	50.9 ± 2.0 (14)	0.35
Intrinsic properties				
$V_{resting}$ (mV)	−78.5 ± 0.9 (28)	−78.5 ± 0.9 (26)	−78.1 ± 0.7 (50)	0.94
R_{input} (MΩ)	194 ± 22 (28)	218 ± 19 (31)	257 ± 15 (51)	0.035[d]
C_m (pF)	45.1 ± 2.5 (28)	49.4 ± 3.2 (31)	36.2 ± 1.8 (51)	0.0003[e]
$V_{threshold}$ (mV)	−38.4 ± 0.9 (15)	−39.6 ± 0.9 (13)	−39.5 ± 0.4 (31)	0.40
$I_{threshold}$ (pA)	127 ± 10 (14)	95.2 ± 7.3 (13)	84.5 ± 5.1 (31)	0.0003[f]

Mean ± SEM is shown, with cell numbers in parentheses. C_m, membrane capacitance; $I_{threshold}$, threshold current for spiking; R_{input}, input resistance; $V_{resting}$, resting potential; $V_{threshold}$, threshold potential for spiking. *Properties shown in the Pup and Adult columns include previously published data (Laplagne *et al*., 2006). [a]*P*-value from one-way ANOVA of embryo vs pup vs adult. If $P < 0.05$, Bonferroni *post-hoc* tests were used to compare all pairs. Only *post hoc* tests with $P < 0.05$ are reported. [b]Two-way ANOVA: row effect (early vs late), $P < 0.0001$; column effect (embryo vs pup vs adult), $P = 0.56$. [c]Two-way ANOVA: row effect (early vs late), $P < 0.0001$; column effect (embryo vs pup vs adult), $P = 0.63$. [d]*Post-hoc* test: embryo vs adult, $P < 0.05$. [e]*Post-hoc* tests: embryo vs adult, $P < 0.05$; pup vs adult, $P < 0.001$. [f]*Post-hoc* tests: embryo vs pup, $P < 0.05$; embryo vs adult, $P < 0.001$.

and threshold current (Table 1). Adult-born cells displayed a lower capacitance, which does not seem to modify their firing properties (Laplagne *et al*., 2006). DGCs born in the embryo displayed a lower input resistance and an increased threshold current for spiking. Overall, these results point to a lower excitability of neurons born during embryonic development, suggesting a possible functional distinction for these cells.

Discussion

Retroviral labeling of dividing progenitors has proven to be a reliable tool for studying the structure and function of DGCs born in the early postnatal and adult mouse brain (van Praag *et al*., 2002; Espósito *et al*., 2005; Ge *et al*., 2006; Laplagne *et al*., 2006; Zhao *et al*., 2006). In the present work we have used this technique to differentially label DGCs born during embryonic development and adulthood. This allowed us to complete our quantitative study of GABAergic inputs on neurons born at all developmental stages.

DGCs receive inhibitory inputs from a complex variety of GABAergic interneurons (Freund & Buzsaki, 1996). Interneuron types can be separated into those innervating the perisomatic domain of principal neurons and those contacting their dendrites. A functional distinction has been proposed, whereby perisomatic inhibition controls axonal output while dendritic inhibition controls dendritic excitability, thus modulating the impact of excitatory afferents (Cobb *et al*., 1995; Miles *et al*., 1996). Measurements on GABAergic synaptic currents thus reflect on the individual properties and relative contributions of inhibitory inputs from a wide variety of interneuron types. After measuring the same properties in all three groups (embryo-, pup- and adult-born DGCs), ANOVAs revealed no significant effect of cell birth date. This is striking considering the broad spectrum of measured properties. For eIPSCs we have studied the amplitude, kinetics, reversal potential and conductance of perisomatic and dendritic

FIG. 3. Spontaneous GABAergic activity. (A) sIPSCs recorded at $V_{Hold} = -80$ mV from an embryo-born DGC. The interval marked by the dashed box is expanded on the bottom. Scale bars: 1 s, 40 pA (top); 50 ms, 40 pA (bottom). (B) sIPSCs recorded at $V_{Hold} = 0$ mV from an embryo-born DGC. The interval marked by the dashed box is expanded on the bottom. Scale bars: 0.5 s, 10 pA (top); 25 ms, 10 pA (bottom). (C and D) sIPSCs recorded as described in (A and B), respectively, were completely blocked by 20 μM bicuculline (BMI; $V_{Hold} = -80$ mV, $n = 3$ cells; $V_{Hold} = 0$ mV, $n = 5$ cells). Scale bars: 10 s, 10 pA. (E and F) Two-dimensional histograms of individual sIPSC kinetics recorded at $V_{Hold} = -80$ mV (C, $n = 3824$ events) and 0 mV (D, $n = 508$ events). The color scale indicates the relative frequency for each bin (square areas in the graph). (G and H) Cumulative histograms of the same events included in (E and F), respectively. (I) Comparison of frequency ($P = 0.007$), rise time ($P < 0.0001$) and decay time ($P < 0.0001$) of sIPSCs recorded at $V_{Hold} = -80$ mV and 0 mV on embryo-born DGCs (**$P < 0.01$ and ***$P < 0.0001$). All experiments were carried out in the presence of 4 mM kyn.

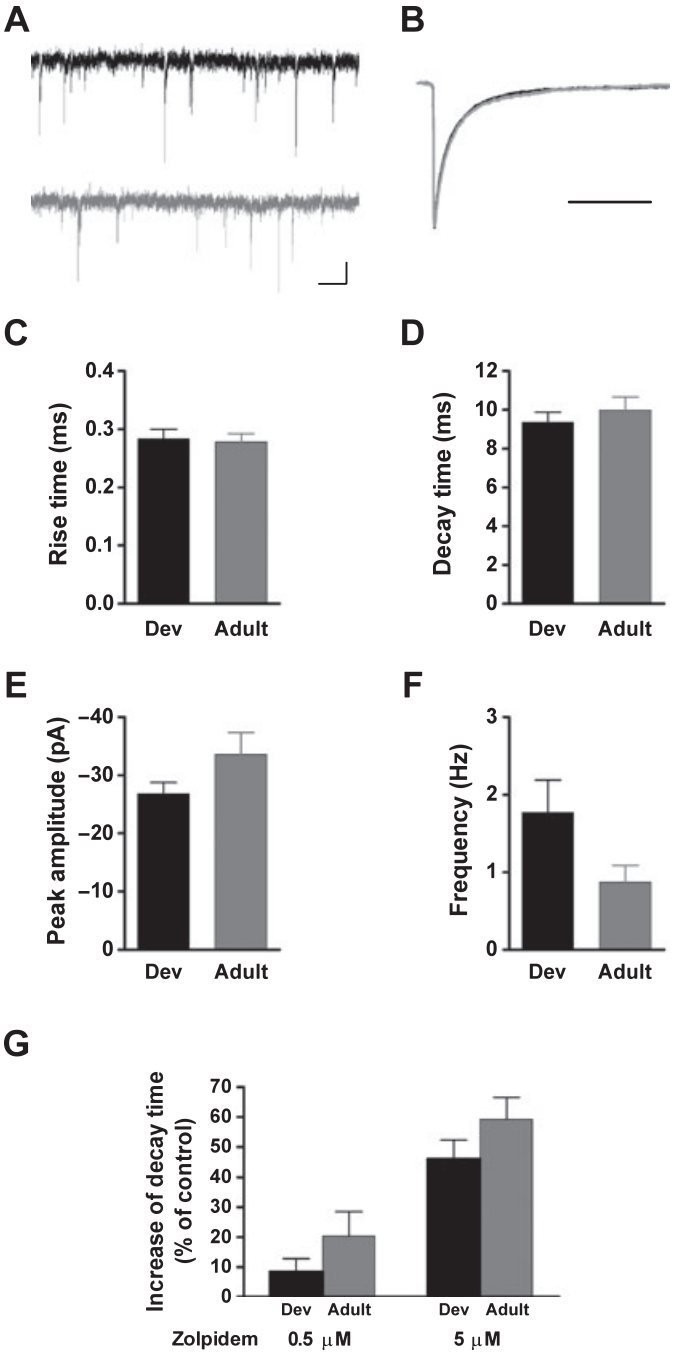

FIG. 4. Miniature GABAergic activity. (A) Examples of mIPSC recordings obtained from neurons born in the developing (top) and adult dentate gyrus (bottom). Scale bars: 1 s, 10 pA. (B) Superimposed scaled averages of mIPSCs recorded from all development- (black trace) and adult-born DGCs (gray trace). Scale bar: 50 ms. (C–F) Rise time 20–80% ($P = 0.81$), decay time 100–60% ($P = 0.47$), peak amplitude ($P = 0.11$) and frequency ($P = 0.10$) of mIPSCs recorded from development- and adult-born DGCs ($n = 12$ and 9 cells, respectively). (G) Increase of decay time (peak to 40%) as a function of zolpidem dose. Values are expressed as percent increase with respect to mean control values measured in the absence of drug. Two-way ANOVA revealed a significant effect of drug dose ($P < 0.0001$) but not cell birth date ($P = 0.07$; $n = 7$–11 for all four groups). All experiments were carried out at $V_{Hold} = -60$ mV in the presence of kyn (4 mM) and TTX (0.5 μM).

afferents. For sIPSCs we have measured the frequency, kinetics and amplitude of events arising at both the soma and the dendrites. Detailed properties of postsynaptic receptors were also examined by mIPSC analysis. Our present observations further substantiate the notion that, although immature neurons display GABAergic inputs that are different from those of mature DGCs, all neurons ultimately converge into an inhibitory connectivity of remarkable similarity (Espósito *et al*., 2005; Overstreet Wadiche *et al*., 2005; Laplagne *et al*., 2006).

This work adds to the current evidence strongly suggesting that DGCs born at all developmental stages contribute to the same functional population after their maturation is complete (van Praag *et al*., 2002; Espósito *et al*., 2005; Laplagne *et al*., 2006). Interestingly, here we observed a lower input resistance and threshold current for spiking in mature neurons born at E15, which underscores their reduced excitability compared with granule cells born at P7 or adulthood (Table 1). At the time when excitability was studied, neurons born in the embryo, pup and adult dentate gyrus were 14, 13 and 7 weeks old, respectively; differences in age could introduce potential sources for differences in function (Schmidt-Hieber *et al*., 2004; Espósito *et al*., 2005; Ge *et al*., 2006; Overstreet-Wadiche *et al*., 2006; Piatti *et al*., 2006). However, DGCs generated in embryo and pup exhibit distinct membrane properties yet are of similar ages at the time of recording. We conclude that strength and distribution of GABAergic afferents do not seem to depend on the age, location or degree of excitability of granule cells but, rather, they might obey to other factors that require further investigation.

The lower excitability found for neurons generated during embryonic development might underscore a decreased engagement in network activity for these neurons, taking into account the overall similarity in the strength and individual properties of GABAergic afferents in all three neuronal populations studied here. However, this might be compensated by stronger excitatory inputs, which have not been characterized here. In addition, how GABAergic afferents impinge on neuronal function will not only depend on the intrinsic membrane properties and excitatory afferents, but also on the impact of additional neurotransmitters and neuromodulators, including neurotrophic factors. In fact, $GABA_B$ receptors can exert a powerful modulation of perforant path afferents during high-frequency stimulation (Wang & Wojtowicz, 1997). Granule cells also receive extrinsic axonal inputs that release acetylcholine, noradrenaline, dopamine and serotonin, to list some examples (Johnston & Amaral, 1998). Their firing behavior will therefore depend on the responsiveness to these modulatory factors. Whether or not any of the three neuronal populations described here are selectively activated in the context of the complex hippocampal circuitry must be determined by *in vivo* studies. A recent study using Arc expression has shown that adult-born DGCs are twice as likely to become active during spatial exploration when compared with neighboring old cells presumably born during perinatal development (Ramirez-Amaya *et al*., 2006). Our current findings underscore the necessity of further investigating putative functional differences in neurons born in the embryonic vs early postnatal dentate gyrus.

As they mature from undifferentiated progenitors to fully developed neurons, adult-born cells have been shown to display distinct intrinsic membrane properties, afferent connectivity and plasticity (Schmidt-Hieber *et al*., 2004; Espósito *et al*., 2005; Ge *et al*., 2006; Overstreet-Wadiche *et al*., 2006; Piatti *et al*., 2006). It has been recently proposed that young DGCs with a higher excitability could aid the temporal binding of memories (Aimone *et al*., 2006). Whether neurons at these immature stages are relevant to the hippocampal network activity remains to be investigated. Functional output from neurons born in the adult brain also awaits experimental evidence, and the neurotransmitter phenotype of these cells is still unknown. Although axons originating from DGCs (the mossy fibers) are classically considered

glutamatergic, a dual GABAergic and glutamatergic phenotype has been reported (Walker *et al*., 2001; Gutierrez, 2005). The possibility remains that, at some maturation stages, adult-born DGCs might release GABA from their terminals. Determining the timing of establishment of functional connections onto target cells and their neurotransmitter phenotype will be necessary to shed light onto current hypotheses on the biological significance of adult neurogenesis.

Acknowledgements

We thank Alysson Muotri for technical advice on intrauterine injections. A.F.S. is an investigator of the Argentine National Research Council (Consejo Nacional de Investigaciones Científicas y Técnicas – CONICET). D.A.L., M.S.E. and V.C.P. were supported by doctoral fellowships from CONICET. This work was supported by the National Institutes of Health – Fogarty International Research Collaboration Award (RO3TW06130-01) to A.F.S. and F.H.G., and grants from Fundación Antorchas and the Agencia Nacional para la Promoción de Ciencia y Tecnología (ANPCyT) to A.F.S.

Abbreviations

ACSF, artificial cerebrospinal fluid; BMI, bicuculline; DGC, dentate granule cell; E, embryonic day; eIPSCs, evoked inhibitory postsynaptic currents; GABA, γ-aminobutyric acid; GCL, granule cell layer; GFP, green fluorescent protein; IPSC, inhibitory postsynaptic current; kyn, kynurenic acid; mIPSC, miniature inhibitory postsynaptic current; ML, molecular layer; P, postnatal day; RFP, red fluorescent protein; sIPSC, spontaneous inhibitory postsynaptic current; TTX, tetrodotoxin; V_{Hold}, holding potential.

References

Aimone, J.B., Wiles, J. & Gage, F.H. (2006) Potential role for adult neurogenesis in the encoding of time in new memories. *Nat. Neurosci.*, **9**, 723–727.

Altman, J. & Bayer, S.A. (1990a) Migration and distribution of two populations of hippocampal granule cell precursors during the perinatal and postnatal periods. *J. Comp. Neurol.*, **301**, 365–381.

Altman, J. & Bayer, S.A. (1990b) Mosaic organization of the hippocampal neuroepithelium and the multiple germinal sources of dentate granule cells. *J. Comp. Neurol.*, **301**, 325–342.

Angevine, J.B. Jr (1965) Time of neuron origin in the hippocampal region. An autoradiographic study in the mouse. *Exp Neurol. Suppl.*, **2**, 1–70.

Bayer, S.A. (1980) Development of the hippocampal region in the rat. I. Neurogenesis examined with 3H-thymidine autoradiography. *J. Comp. Neurol.*, **190**, 87–114.

Campbell, R.E., Tour, O., Palmer, A.E., Steinbach, P.A., Baird, G.S., Zacharias, D.A. & Tsien, R.Y. (2002) A monomeric red fluorescent protein. *Proc. Natl Acad. Sci. USA*, **99**, 7877–7882.

Cobb, S.R., Buhl, E.H., Halasy, K., Paulsen, O. & Somogyi, P. (1995) Synchronization of neuronal activity in hippocampus by individual GABAergic interneurons. *Nature*, **378**, 75–78.

De Koninck, Y. & Mody, I. (1994) Noise analysis of miniature IPSCs in adult rat brain slices: properties and modulation of synaptic GABAA receptor channels. *J. Neurophysiol.*, **71**, 1318–1335.

Espósito, M.S., Piatti, V.C., Laplagne, D.A., Morgenstern, N.A., Ferrari, C.C., Pitossi, F.J. & Schinder, A.F. (2005) Neuronal differentiation in the adult hippocampus recapitulates embryonic development. *J. Neurosci.*, **25**, 10074–10086.

Freund, T.F. & Buzsaki, G. (1996) Interneurons of the hippocampus. *Hippocampus*, **6**, 347–470.

Ge, S., Goh, E.L., Sailor, K.A., Kitabatake, Y., Ming, G.L. & Song, H. (2006) GABA regulates synaptic integration of newly generated neurons in the adult brain. *Nature*, **439**, 589–593.

Gutierrez, R. (2005) The dual glutamatergic-GABAergic phenotype of hippocampal granule cells. *Trends Neurosci.*, **28**, 297–303.

Hollrigel, G.S. & Soltesz, I. (1997) Slow kinetics of miniature IPSCs during early postnatal development in granule cells of the dentate gyrus. *J. Neurosci.*, **17**, 5119–5128.

Jarolimek, W., Lewen, A. & Misgeld, U. (1999) A furosemide-sensitive K+-Cl- cotransporter counteracts intracellular Cl- accumulation and depletion in cultured rat midbrain neurons. *J. Neurosci.*, **19**, 4695–4704.

Johnston, D. & Amaral, D.G. (1998) Hippocampus. In Shepherd, G.M. (Ed.), *The Synaptic Organization of the Brain.* Oxford University Press, New York, pp. 417–458.

Kaila, K. (1994) Ionic basis of GABAA receptor channel function in the nervous system. *Prog. Neurobiol.*, **42**, 489–537.

Kempermann, G., Gast, D., Kronenberg, G., Yamaguchi, M. & Gage, F.H. (2003) Early determination and long-term persistence of adult-generated new neurons in the hippocampus of mice. *Development*, **130**, 391–399.

Laplagne, D.A., Espósito, M.S., Piatti, V.C., Morgenstern, N.A., Zhao, C., van Praag, H., Gage, F.H. & Schinder, A.F. (2006) Functional convergence of neurons generated in the developing and adult hippocampus. *PLoS Biol.*, **4**, e409.

Mathews, E.A., Morgenstern, N., Piatti, V., Jessberger, S., Schinder, A. & Gage, F.H. (2006) Developmental layering to mouse dentate gyrus through adult neurogenesis. *Soc. Neurosci. Abstr.*, **32**, 419.9.

Miles, R., Toth, K., Gulyas, A.I., Hajos, N. & Freund, T.F. (1996) Differences between somatic and dendritic inhibition in the hippocampus. *Neuron*, **16**, 815–823.

Overstreet Wadiche, L.S., Bromberg, D.A., Bensen, A.L. & Westbrook, G.L. (2005) GABAergic signaling to newborn neurons in dentate gyrus. *J. Neurophysiol.*, **94**, 4528–4532.

Overstreet-Wadiche, L.S., Bensen, A.L. & Westbrook, G.L. (2006) Delayed development of adult-generated granule cells in dentate gyrus. *J. Neurosci.*, **26**, 2326–2334.

Pearce, R.A. (1993) Physiological evidence for two distinct $GABA_A$ responses in rat hippocampus. *Neuron*, **10**, 189–200.

Piatti, V.C., Esposito, M.S. & Schinder, A.F. (2006) The timing of neuronal development in adult hippocampal neurogenesis. *Neuroscientist*, **12**, 463–468.

van Praag, H., Schinder, A.F., Christie, B.R., Toni, N., Palmer, T.D. & Gage, F.H. (2002) Functional neurogenesis in the adult hippocampus. *Nature*, **415**, 1030–1034.

Ramirez-Amaya, V., Marrone, D.F., Gage, F.H., Worley, P.F. & Barnes, C.A. (2006) Integration of new neurons into functional neural networks. *J. Neurosci.*, **26**, 12237–12241.

Schlessinger, A.R., Cowan, W.M. & Gottlieb, D.I. (1975) An autoradiographic study of the time of origin and the pattern of granule cell migration in the dentate gyrus of the rat. *J. Comp. Neurol.*, **159**, 149–175.

Schlessinger, A.R., Cowan, W.M. & Swanson, L.W. (1978) The time of origin of neurons in Ammon's horn and the associated retrohippocampal fields. *Anat. Embryol. (Berl.)*, **154**, 153–173.

Schmidt-Hieber, C., Jonas, P. & Bischofberger, J. (2004) Enhanced synaptic plasticity in newly generated granule cells of the adult hippocampus. *Nature*, **429**, 184–187.

Snyder, J.S., Kee, N. & Wojtowicz, J.M. (2001) Effects of adult neurogenesis on synaptic plasticity in the rat dentate gyrus. *J. Neurophysiol.*, **85**, 2423–2431.

Soltesz, I., Smetters, D.K. & Mody, I. (1995) Tonic inhibition originates from synapses close to the soma. *Neuron*, **14**, 1273–1283.

Stell, B.M. & Mody, I. (2002) Receptors with different affinities mediate phasic and tonic GABA(A) conductances in hippocampal neurons. *J. Neurosci.*, **22**, RC223.

Walker, M.C., Ruiz, A. & Kullmann, D.M. (2001) Monosynaptic GABAergic signaling from dentate to CA3 with a pharmacological and physiological profile typical of mossy fiber synapses. *Neuron*, **29**, 703–715.

Wang, S., Scott, B.W. & Wojtowicz, J.M. (2000) Heterogenous properties of dentate granule neurons in the adult rat. *J. Neurobiol.*, **42**, 248–257.

Wang, S. & Wojtowicz, J.M. (1997) Effects of GABAB receptors on synaptic interactions in dentate gyrus granule neurons of the rat. *Neuroscience*, **79**, 117–127.

Zhao, C., Teng, E.M., Summers, R.G. Jr, Ming, G.L. & Gage, F.H. (2006) Distinct morphological stages of dentate granule neuron maturation in the adult mouse hippocampus. *J. Neurosci.*, **26**, 3–11.